Structural Engineering and Mechanics, Vol. 43, No. 2 (2012) 253-271
DOI: http://dx.doi.org/10.12989/sem.2012.43.2.253

A new higher-order triangular plate bending element for the analysis of laminated composite and sandwich plates

M. Rezaiee-Pajand*, F. Shahabian and F.H. Tavakoli

Department of Civil Engineering, Ferdowsi University of Mashhad, Mashhad 1111-9775, Iran

(Received February 16, 2012, Revised May 15, 2012, Accepted June 1, 2012)

Abstract. To analyze the bending and transverse shear effects of laminated composite plates, a thirteen nodes triangular element will be presented. The suggested formulations consider a parabolic variation of the transverse shear strains through the thickness. As a result, there is no need to use shear correction coefficients in computing the shear stresses. The proposed element can model both thin and thick plates without any problems, such as shear locking and spurious modes. Moreover, the effectiveness of $w_{,n}$, as an independent degree of freedom, is concluded by the present study. To perform the accuracy tests, several examples will be solved. Numerical results for the orthotropic materials with different boundary conditions, shapes, number of layers, thickness ratios and fiber orientations will be presented. The suggested element calculates the deflections and stresses more accurate than those available in the literature.

Keywords: plate bending; laminate; finite element analysis (FEA); shear deformation, thin and thick plates.

1. Introduction

In the recent decades, composite materials have extensively been used for a number of applications in various fields, such as civil, mechanical and aerospace engineering. Composite laminates are widely utilized in structures due to their lightweight, high ratios of stiffness and strength to weight. Furthermore, these materials have suitable sound absorption and flexibility for use in complex structural configurations. Finite element analysis of laminate composite plates in the recent decades has been mainly based on four plate theories. These theories include: the classical lamination theory (CLT) based on Kirchhoff hypothesis, first-order shear deformation theory (FSDT), higher-order shear deformation theory (HSDT) and layer-wise lamination theory (Reddy 1997, Timoshenko and Krieger 1959, Reissner 1945, Mindlin 1951). The CLT is an extension of the classical thin plate theory to laminated plates, which neglects the effects of transverse shear and requires continuity of the deflections and their slopes (C^1 continuity) in displacement fields. The errors in the CLT theory increase as the thickness-span ratio of plate increases.

The first-order shear deformation theories (FSDT) are based on Reissner-Mindlin plate theory (Rezaiee-Pajand and Sarafrazi 2000). FSDT theories only require C^0 continuity, and they can be

*Corresponding author, Professor, E-mail: mrpajand@yahoo.com

used for the analysis of both thick and thin plates. In FSDT, the transverse shearing strains or stresses are assumed constant through the plate thickness. This is not agreeing with the zero shear stress conditions on the bounding planes of the plate, and several spurious shear correction coefficients must be introduced (Cen *et al.* 2002). The displacement finite element techniques tend to cause undesirable shear locking phenomena for low order interpolation polynomials in Reissner-Mindlin elements. Locking effect occurs by the selective integration methods. These techniques in some occasions lead to the appearance of spurious mechanisms. The use of mixed interpolations has been adopted as the more popular alternative to the selective method where the deflection, the rotations and the shear forces are independently interpolated (Belounar and Guenfoud 2005). Higher-order plate theories have been proposed by some researchers. Taking advantage of free parameters in the stiffness matrix and optimizing the element behavior by template strategy can improve the structural responses (Rezaiee-Pajand and Mohamadzade 2010). Another way of increasing the element accuracy is using hybrid-Trefftz formulations for plate bending analysis (Rezaiee-Pajand and Karkon 2012).

Two different methods have been commonly employed that include single-layer and multi-layer formulations. The former increases the order considered for the displacement representation in the thickness coordinate, and the latter assumes a representation formula for the displacement field in each layer, similar to that of layer-wise theory. Carrera *et al.* (2011) compared the solutions obtained via equivalent single-layer fourth-order FEM model and a layer-wise one and investigated the sets of effective terms for a different length-to-thickness ratio in the case of an unsymmetrical cross-ply square simply-supported plate under a distributed load.

Some Techniques have been presented to solve the mentioned problems of the FSDT. For instance, the distribution of transverse shear stresses can be evaluated by a three-dimensional (3D) elasticity equilibrium equation. Vlachoutsis (1992) proposed a simple approach to calculate shear correction factors for laminated plates and shells under cylindrical bending. Rolfes and Rohwer (1997) studied a simple post-processing procedure to obtain improved transverse shear stresses in the finite element analysis based on FSDT. Rolfes *et al.* (1998) suggested a simple and accurate post-processing method for the FSDT to calculate the transverse normal stress, which was initially assumed to be zero. During the past 40 years, many researchers have made significant contributions on development of simple triangular and quadrilateral elements based on FSDT (Cen *et al.* 2002).

A considerable work has been done on the composites in the last decade. For example, Polit and Touratier (2000) formulated a new C^1 six-node triangular finite element for geometrically linear and non-linear elastic multilayered composite plates. This finite element could model both thin and thick plates without any shear locking and spurious modes and was built on the Argyris interpolation for bending and the new interpolation type for membrane displacements and transverse shear rotations. Sheikh *et al.* (2002) developed a high precision triangular element for the analysis of laminated composite plates. In this element, the effect of shear deformation was considered by taking transverse displacement and bending rotations as independent field variables. Cen *et al.* (2002) presented a simple displacement based, quadrilateral 20 DOF bending element based on the first-order shear deformation theory for analysis of composite plates. Their element was constructed by two procedures. First, the variation functions of the rotation and the shear strain along each side of the element were determined using Timoshenko's beam theory and second the shear strain, rotation and in-plane displacement fields in the domain of the element were determined using the technique of improved interpolation. Furthermore, a simple hybrid procedure was also proposed to improve the stress solutions.

Sheikh and Chakrabartib (2003) proposed a triangular element based on Reddy's higher-order shear deformation plate theory. The transverse displacement was approximated by a truncated quintic polynomial. That was obtained by imposing cubic variation of normal slope along the three sides, which had helped to express the three unknowns of a complete quintic polynomial in terms of other unknowns. Belounar and Guenfoud (2005) presented a new four nodes rectangular finite element for the linear analysis of plate bending with transverse shear effect. The related displacement fields were developed using the strain-based approach, and it was based on the assumed independent functions for the various components of strain in so far as it was allowed by the compatibility equations. Belinha and Dinis (2006) extended a meshless method (the element-free Galerkin method (EFGM)) and used in the analysis of anisotropic plates and laminates considering a Reissner-Mindlin laminate theory (FSDT). The approximation functions were calculated considering the moving least squares (MLS) approach, which was consistent provided the basis was complete in the polynomials up to a desired order. Shear locking in plate bending was avoided considering the appropriate polynomials for the displacements and rotations. Cai *et al.* (2008) developed a small strain and elasto-plastic formulation of Polygonal Element Method (PEM) for efficient analysis of elasto-plastic solids. The construction method of polygonal mesh can directly utilize the sophisticated triangularization algorithm and reduce the difficulty in generating polygonal elements. The incremental variational form and a Von-Mises type model were used for non-linear elasto-plastic analysis.

Dash and Singh (2010) proposed a transverse bending of shear deformable laminated composite plates in Green-Lagrange sense accounting for the transverse shear and large rotations. Governing equations were developed in the framework of higher-order shear deformation method. Their theory satisfied zero transverse shear strains conditions at the top and bottom surfaces of the plate in von-Karman sense. A C^0 isoparametric finite element was developed for the proposed nonlinear model. Zhen and Wanji (2010) developed a C^0-type higher-order theory for bending analysis of laminated composite and sandwich plates subjected to thermal-mechanical loads. The total number of unknowns in this theory was independent of the number of layers. Thinh and Quoc (2010) studied free vibration and bending failure of laminated stiffened glass fiber-polyester composite plates with laminated open section (rectangular or T-shaped) and closed section (hat shaped) of stiffeners by finite element method and experiment. Tu *et al.* (2010) extended a nine-nodded rectangular element with nine degrees of freedom at each node for the bending and vibration analysis of laminated and sandwich composite plates. The theory accounted for parabolic distribution of the transverse shear strains through thickness of the plate and rotary inertia effects.

Alieldin *et al.* (2011) presented the first-order shear deformation plate (FSDT) model to investigate the mechanical behavior of laminated composite and functional graded plates. Three procedures developed to transform the laminated composite plate, with stepped material properties, to an equivalent functionally graded (FG) plate with a continuous property function across the plate thickness. Bussamra *et al.* (2012) proposed three-dimensional hybrid finite elements for the analysis of laminated composite plates. Two independent fields were approximated: stresses within the elements and displacements on their boundary. The required stress field in point-wise equilibrium was generated by harmonic and orthogonal polynomials with the potentials to generate homogeneous solution of Navier equations for isotropic material. Notably, based on the presented brief review, the HSDT methods are able to produce overall global response and in-plane stresses with reasonable accuracy and less computational effort, besides their simplicity over the layer-wise and zigzag models.

In this paper, a new higher-order thirteen nodes triangular bending element, which includes transverse shear effect, is generalized for analyzing multilayered anisotropic composite plates. The principle of minimum potential energy is introduced to establish the relationship between the displacement and the stress or internal force fields. Extensive finite element analyses were performed by utilizing the author's computer program, which includes the proposed higher-order shear deformation element. Good results were obtained in comparison to the other available finite elements. Moreover, the effectiveness of $w_{,n}$, as an independent degree of freedom, is concluded by the present study. Due to the page limit, only a few of the numerical examples are given in this paper. However, it will be clearly illustrated that the new higher-order element possesses the advantages of displacement-based elements, such as simple formulas for solving displacements with high precision and rational distributions. Besides, the suggested formulations lead to both accurate solutions for stresses and internal forces.

2. Finite element modeling

At this stage, a triangular bending element with transverse shear effect will be formulated in details. The suggested element is very useful for the modeling of the laminated composite plates. Rezaiee-Pajand and Akhtary (1996, 1998) suggested several plate bending triangular elements in order to investigate the effect of elemental degrees of freedom in isotropic plates. All of these elements were not C^1 compatible, and their related nodes had various degrees of freedom. Kirchhoff's theory was used for finite element analysis of thin plate bending. They concluded that the T13-5 element was the best one. This element had 13 nodes, which were located at the corners and centroid, and also there were three nodes in each side. The related degrees of freedom for the element were: w, $w_{,x}$ and $w_{,y}$ on the corners and centroid, w in the mid-side and $w_{,n}$ in other nodes. It should be added that, although the other proposed elements had 13 nodes and with the same displacement function, their degrees of freedom were not very effective (Rezaiee-Pajand and Akhtary 1998). In the following sections, a higher-order triangular plate bending element for the analysis of laminated composite plates is developed, which has thirteen nodes. Furthermore, a computer program which can utilize the presented formulation is prepared by the authors.

2.1 A triangular element with 13 nodes

The proposed formulation is based on higher-order shear deformation plate theory. It is assumed that the transverse displacement is small compared to plate thickness, and the plate material follows Hooke's law. Locations of the element nodes discussed in this paper are shown in Fig. 1. Deflection of the plate (w) and its derivatives are the degrees of freedom used in this study. There are two types of coordinates for this element: Cartesian coordinates (x, y), which are used for any nodes, and (t, n) coordinates, which are used for mid-side nodes. The mentioned coordinates are shown in Fig. 2. The following relationships exist between x, y, n and t coordinates

$$\begin{cases} n = Cx + Sy \\ t = -Sx + Cy \end{cases}, \qquad \begin{cases} C = \cos\theta \\ S = \sin\theta \end{cases} \tag{1}$$

Several types of degrees of freedom are used in this study. The first and second derivatives of w,

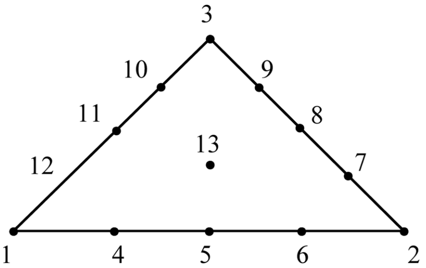

Fig. 1 Triangular element with 13 nodes

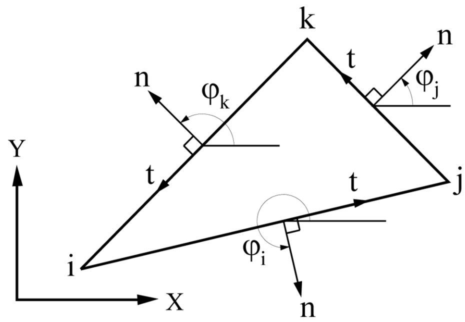

Fig. 2 Element coordinates

with respect to x, y and n are utilized. All degrees of freedom for the suggested element are displacement components (u, v, w), bending rotations (θ_x, θ_y) and partial derivative of w with respect to n ($\partial w/\partial n$). This triangular element uses u, v, w, w_x and w_y as degrees of freedom for nodes 1, 2, 3 and 13, and u, v, w, w_x, w_y and $w_{,n}$ for nodes 4, 6, 7, 9, 10 and 12. In addition to these, nodal deflection, w, is utilized for nodes 5, 8 and 11, as a degree of freedom.

In this study, a fifth-order polynomial is used for the transverse displacement (w) and forth-order polynomial is used for displacement components (u, v), bending rotations (θ_x, θ_y) and partial derivative of w with respect to n ($\partial w/\partial n$). These functions have the following form

$$u = [N_1]\{\alpha\}, \quad v = [N_1]\{\beta\}, \quad w = [N_2]\{\gamma\} \tag{2}$$

$$\theta_x = [N_1]\{\lambda\}, \quad \theta_y = [N_1]\{\mu\}, \quad \partial w/\partial n = [N_1]\{\psi\} \tag{3}$$

$$[N_1] = [1 \ \xi_i^4 \ \xi_i^3\xi_j \ \xi_i^3\xi_k \ \xi_i^2\xi_j^2 \ \xi_i^2\xi_k^2 \ \xi_i^2\xi_j\xi_k \ \xi_i\xi_j^3 \ \xi_i\xi_k^3 \ \xi_i\xi_j^2\xi_k \ \xi_i\xi_j\xi_k^2 \ \xi_j^4 \ \xi_j^3\xi_k \ \xi_j^2\xi_k^2 \ \xi_j\xi_k^3 \ \xi_k^4] \tag{4}$$

$$\begin{aligned}[N_2] = [1 \ &\xi_i^5 \ \xi_i^4\xi_j \ \xi_i^4\xi_k \ \xi_i^3\xi_j^2 \ \xi_i^3\xi_j\xi_k \ \xi_i^3\xi_k^2 \ \xi_i^2\xi_j^3 \ \xi_i^2\xi_j^2\xi_k \ \xi_i^2\xi_j\xi_k^2 \ \xi_i^2\xi_k^3 \ \xi_i\xi_j^4 \\ &\xi_i\xi_j^3\xi_k \ \xi_i\xi_j^2\xi_k^2 \ \xi_i\xi_j\xi_k^3 \ \xi_i\xi_k^4 \ \xi_j^5 \ \xi_j^4\xi_k \ \xi_j^3\xi_k^2 \ \xi_j^2\xi_k^3 \ \xi_j\xi_k^4 \ \xi_k^5]\end{aligned} \tag{5}$$

$$\{\alpha\} = \{\alpha_1 \ \alpha_2 \ \alpha_3 \ \alpha_4 \ \alpha_5 \ \alpha_6 \ \alpha_7 \ \alpha_8 \ \alpha_9 \ \alpha_{10} \ \alpha_{11} \ \alpha_{12} \ \alpha_{13} \ \alpha_{14} \ \alpha_{15} \ \alpha_{16}\}^T \tag{6}$$

$$\{\beta\} = \{\beta_1 \ \beta_2 \ \beta_3 \ \beta_4 \ \beta_5 \ \beta_6 \ \beta_7 \ \beta_8 \ \beta_9 \ \beta_{10} \ \beta_{11} \ \beta_{12} \ \beta_{13} \ \beta_{14} \ \beta_{15} \ \beta_{16}\}^T \tag{7}$$

$$\{\gamma\} = \{\gamma_1 \ \gamma_2 \ \gamma_3 \ \gamma_4 \ \gamma_5 \ \gamma_6 \ \gamma_7 \ \gamma_8 \ \gamma_9 \ \gamma_{10} \ \gamma_{11} \ \gamma_{12} \ \gamma_{13} \ \gamma_{14} \ \gamma_{15} \ \gamma_{16} \ \gamma_{17} \ \gamma_{18} \ \gamma_{19} \ \gamma_{20} \ \gamma_{21} \ \gamma_{22}\}^T \tag{8}$$

$$\{\lambda\} = \{\lambda_1 \ \lambda_2 \ \lambda_3 \ \lambda_4 \ \lambda_5 \ \lambda_6 \ \lambda_7 \ \lambda_8 \ \lambda_9 \ \lambda_{10} \ \lambda_{11} \ \lambda_{12} \ \lambda_{13} \ \lambda_{14} \ \lambda_{15} \ \lambda_{16}\}^T \tag{9}$$

$$\{\mu\} = \{\mu_1 \ \mu_2 \ \mu_3 \ \mu_4 \ \mu_5 \ \mu_6 \ \mu_7 \ \mu_8 \ \mu_9 \ \mu_{10} \ \mu_{11} \ \mu_{12} \ \mu_{13} \ \mu_{14} \ \mu_{15} \ \mu_{16}\}^T \tag{10}$$

$$\{\psi\} = \{\psi_1 \ \psi_2 \ \psi_3 \ \psi_4 \ \psi_5 \ \psi_6 \ \psi_7 \ \psi_8 \ \psi_9 \ \psi_{10} \ \psi_{11} \ \psi_{12} \ \psi_{13} \ \psi_{14} \ \psi_{15} \ \psi_{16}\}^T \tag{11}$$

In these equations, dimensionless vectors ξ_i, ξ_j and ξ_k vary from zero to one in all triangular intervals. To express the unknown coefficients of the assumed polynomials in terms of the nodal displacement vector, $\{\delta\}$, the field variables may be determined appropriately by the following equations

$$\{\delta\} = [A]\{\Delta\} \quad \text{or} \quad \{\Delta\} = [A]^{-1}\{\delta\} \tag{12}$$

$$\{\Delta\} = [[\alpha]^T \; [\beta]^T \; [\gamma]^T \; [\lambda]^T \; [\mu]^T \; [\psi]^T] \tag{13}$$

$$\begin{aligned}\{\delta\}^T = [&u_1 \; v_1 \; w_1 \; \theta_{x1} \; \theta_{y1} \; u_2 \; v_2 \; w_2 \; \theta_{x2} \; \theta_{y2} \; u_3 \; v_3 \; w_3 \; \theta_{x3} \; \theta_{y3} \\ &u_4 \; v_4 \; w_4 \; \theta_{x4} \; \theta_{y4} \; w_{4,n} \; w_5 \; u_6 \; v_6 \; w_6 \; \theta_{x6} \; \theta_{y6} \; w_{6,n} \; u_7 \\ &v_7 \; w_7 \; \theta_{x7} \; \theta_{y7} \; w_{7,n} \; w_8 \; u_9 \; v_9 \; w_9 \; \theta_{x9} \; \theta_{y9} \; w_{9,n} \; u_{10} \; v_{10} \\ &w_{10} \; \theta_{x10} \; \theta_{y10} \; w_{10,n} \; w_{11} \; u_{12} \; v_{12} \; w_{12} \; \theta_{x12} \; \theta_{y12} \; w_{12,n} \; u_{13} \; v_{13} \; w_{13} \; \theta_{x13} \; \theta_{y13}]\end{aligned} \tag{14}$$

In the last formulas, $w_{,n}$ is the normal vector associated to *j-k* side of the triangular element that is shown in Fig. 2. This partial derivative of w with respect to n can be written in the form bellow

$$w_{,n_j} = \frac{\partial w}{\partial n_j} = \frac{\partial w}{\partial x}\frac{\partial x}{\partial n_j} + \frac{\partial w}{\partial y}\frac{\partial y}{\partial n_j} = \frac{\partial w}{\partial x}\cos\varphi_j + \frac{\partial w}{\partial y}\sin\varphi_j \tag{15}$$

$$\frac{\partial w}{\partial n_j} = \begin{bmatrix}\frac{\partial w}{\partial x} & \frac{\partial w}{\partial y}\end{bmatrix}\{n_j\} \tag{16}$$

$$\{n_j\} = \pm\begin{Bmatrix}\cos\varphi_j \\ \sin\varphi_j\end{Bmatrix} = \pm\frac{1}{\sqrt{(x_k - x_j)^2 + (y_k - y_j)^2}}\begin{Bmatrix}y_k - y_j \\ x_j - x_k\end{Bmatrix} \tag{17}$$

Where, φ_j is the angle between n_j and x axis. The matrix $[A]$ can be formed with the coordinates of the different nodes. The bending rotations, θ_x and θ_y, are taken as independent field variables, they are not derivations of w. Therefore, the average transverse shear strains can be defined by the following relation

$$\begin{Bmatrix}\phi_x \\ \phi_y\end{Bmatrix} = \begin{Bmatrix}\theta_x - \partial w/\partial x \\ \theta_y - \partial w/\partial y\end{Bmatrix} \tag{18}$$

In the former equation, ϕ_x and ϕ_y are the effects of shear deformations. The interpolation function that is used for transverse displacement (w), in Eq. (18) is one order higher than that used for bending rotations (θ_x, θ_y). This assumption causes the element to be free from shear locking. Eq. (18) can be written in dimensionless coordinates as follows

$$\phi_x = \theta_x - \frac{\partial w}{\partial x} = [N_1]\{\lambda\} - \left(\frac{\partial w}{\partial \xi_i}\frac{\partial \xi_i}{\partial x} + \frac{\partial w}{\partial \xi_j}\frac{\partial \xi_j}{\partial x} + \frac{\partial w}{\partial \xi_k}\frac{\partial \xi_k}{\partial x}\right) \tag{19}$$

$$\phi_y = \theta_y - \frac{\partial w}{\partial y} = [N_1]\{\mu\} - \left(\frac{\partial w}{\partial \xi_i}\frac{\partial \xi_i}{\partial y} + \frac{\partial w}{\partial \xi_j}\frac{\partial \xi_j}{\partial y} + \frac{\partial w}{\partial \xi_k}\frac{\partial \xi_k}{\partial y}\right) \tag{20}$$

The displacement components of a point at a distance of z from the reference plane are given below (Reddy 1984)

$$u(x,y,z) = u_0 + z\left[\theta_x - \frac{4}{3}\left(\frac{z}{h}\right)^2\left(\theta_x + \frac{\partial w}{\partial x}\right)\right] \tag{21}$$

$$v(x,y,z) = v_0 + z\left[\theta_y - \frac{4}{3}\left(\frac{z}{h}\right)^2\left(\theta_y + \frac{\partial w}{\partial y}\right)\right] \tag{22}$$

$$w(x,y,z) = w \tag{23}$$

In these equations, the transverse shear strains have a parabolic variation along z, and they are zero both at the top and bottom of the plate. In this theory, there is no parameter in the formulations, which does not have any physical meaning. The strains resulting from bending in terms of the rotations, θ_x, θ_y and of the mid-surface displacement, u_0, v_0, w, are written in the following form (Reddy 1984)

$$\varepsilon_x = \frac{\partial u_0}{\partial x} + z\frac{\partial \theta_x}{\partial x} - z^3\frac{4}{3h^2}\left(\frac{\partial \theta_x}{\partial x} + \frac{\partial^2 w}{\partial x^2}\right) \tag{24}$$

$$\varepsilon_y = \frac{\partial v_0}{\partial y} + z\frac{\partial \theta_y}{\partial y} - z^3\frac{4}{3h^2}\left(\frac{\partial \theta_y}{\partial y} + \frac{\partial^2 w}{\partial y^2}\right) \tag{25}$$

$$\gamma_{yz} = \theta_y + \frac{\partial w}{\partial y} - z^2\frac{4}{h^2}\left(\theta_y + \frac{\partial w}{\partial y}\right) \tag{26}$$

$$\gamma_{xz} = \theta_x + \frac{\partial w}{\partial x} - z^2\frac{4}{h^2}\left(\theta_x + \frac{\partial w}{\partial x}\right) \tag{27}$$

$$\gamma_{xy} = \frac{\partial u_0}{\partial y} + \frac{\partial v_0}{\partial x} + z\left(\frac{\partial \theta_x}{\partial y} + \frac{\partial \theta_y}{\partial x}\right) - z^3\frac{4}{3h^2}\left(\frac{\partial \theta_x}{\partial y} + \frac{\partial \theta_y}{\partial x} + 2\frac{\partial^2 w}{\partial_x \partial_y}\right) \tag{28}$$

At this stage, the generalized Hooke's law is utilized to obtain the constitutive equations for a layer of orthotropic material. For a plate of constant thickness, composed of thin layers, the following relations are held

$$\begin{Bmatrix} \sigma_x \\ \sigma_y \\ \tau_{xy} \end{Bmatrix} = \begin{bmatrix} Q_{11} & Q_{12} & Q_{16} \\ Q_{12} & Q_{22} & Q_{26} \\ Q_{16} & Q_{26} & Q_{66} \end{bmatrix} \begin{Bmatrix} \varepsilon_x \\ \varepsilon_y \\ \gamma_{xy} \end{Bmatrix}, \quad \begin{Bmatrix} \tau_{xz} \\ \tau_{yz} \end{Bmatrix} = \begin{bmatrix} Q_{44} & Q_{45} \\ Q_{45} & Q_{55} \end{bmatrix} \begin{Bmatrix} \gamma_{xz} \\ \gamma_{yz} \end{Bmatrix} \tag{29}$$

The stress and strain equations have the form below

$$\{\sigma_b\} = \{\sigma_x \ \ \sigma_y \ \ \tau_{xy}\}^T, \quad \{\varepsilon_b\} = \{\varepsilon_x \ \ \varepsilon_y \ \ \gamma_{xy}\}^T, \quad \{\sigma_b\} = [Q_b]\{\varepsilon_b\} \tag{30}$$

$$\{\sigma_s\} = \{\tau_{xz} \ \ \tau_{yz}\}^T, \quad \{\varepsilon_s\} = \{\gamma_{xz} \ \ \gamma_{yz}\}^T, \quad \{\sigma_s\} = [Q_s]\{\varepsilon_s\} \tag{31}$$

The stresses and its associated principle ones are computed for each element at each integration point. The transformed material constants, $[Q_b]$ and $[Q_s]$, can be evaluated with the respect to material properties, such as E_1, E_2, E_3 ν_{12}, ν_{13}, ν_{23}, G_{12}, G_{13}, G_{23} and fiber orientation of the lamina.

Moreover, the rigidity matrix of a laminate, $[D]$, can be described as follows

$$[D] = \begin{bmatrix} [D_b] & 0 \\ 0 & [D_s] \end{bmatrix} \tag{32}$$

Where, $[D_b]$ and $[D_s]$ are the rigidity matrices for bending and shear, respectively. These matrices can be expressed in the bellow form

$$[D_b] = \begin{bmatrix} \begin{bmatrix} A_{11} & A_{12} & A_{16} \\ & A_{22} & A_{26} \\ \text{sym.} & & A_{66} \end{bmatrix} & \begin{bmatrix} B_{11} & B_{12} & B_{16} \\ & B_{22} & B_{26} \\ \text{sym.} & & B_{66} \end{bmatrix} & \begin{bmatrix} E_{11} & E_{12} & E_{16} \\ & E_{22} & E_{26} \\ \text{sym.} & & E_{66} \end{bmatrix} \\ & \begin{bmatrix} D_{11} & D_{12} & D_{16} \\ & D_{22} & D_{26} \\ \text{sym.} & & D_{66} \end{bmatrix} & \begin{bmatrix} F_{11} & F_{12} & F_{16} \\ & F_{22} & F_{26} \\ \text{sym.} & & F_{66} \end{bmatrix} \\ \text{sym.} & & \begin{bmatrix} H_{11} & H_{12} & H_{16} \\ & H_{22} & H_{26} \\ \text{sym.} & & H_{66} \end{bmatrix} \end{bmatrix} \tag{33}$$

$$[D_s] = \begin{bmatrix} \begin{bmatrix} A_{44} & A_{45} \\ \text{sym.} & A_{55} \end{bmatrix} & \begin{bmatrix} D_{44} & D_{45} \\ \text{sym.} & D_{55} \end{bmatrix} \\ \text{sym.} & \begin{bmatrix} F_{44} & F_{45} \\ \text{sym.} & F_{55} \end{bmatrix} \end{bmatrix} \tag{34}$$

The rigidity matrix of a laminate, $[D]$, is constituted with the contributions of its individual lamina. Having matrices $[Q_b]$ and $[Q_s]$, the different quantities of the rigidity matrices, $[D_b]$ and $[D_s]$, can be calculated by the following relationships (Sheikh and Chakrabarti 2003)

$$(A_{ij}, B_{ij}, D_{ij}, E_{ij}, F_{ij}, H_{ij}) = \int_{-h/2}^{h/2} Q_{ij}(1, z, z^2, z^3, z^4, z^6)dz, \quad (i,j = 1, 2, 6) \tag{35}$$

$$(A_{ij}, D_{ij}, F_{ij}) = \int_{-h/2}^{h/2} Q_{ij}(1, z^2, z^4)dz, \quad (i,j = 4, 5) \tag{36}$$

The strain vector, $\{\varepsilon\}$, can be written in terms of the nodal displacement vector $\{\delta\}$, by the following equation

$$\{\varepsilon\} = [B]\{\delta\} \tag{37}$$

Where, $[B]$ is the strain displacement matrix. Following the well-known approach for displacement type finite element, the virtual work technique, the stiffness matrix for the plate element can be expressed as

$$V = \int \{\varepsilon\}^T [D] \{\varepsilon\} dxdy - \int wp dxdy \tag{38}$$

$$[K] = \int_A [B]^T [D][B] dxdy \tag{39}$$

$$[K]\{\delta\} = \{P\} \tag{40}$$

In the last equation, p, $[k]$ and $\{P\}$ are the transverse load of intensity p, the element stiffness matrix and the nodal load vector, respectively. The stiffness matrix recoveries are performed by integration.

3. Numerical examples and discussion

Some problems will be analyzed in this section to show the applications of the proposed element. A computer program is written by the authors to utilize the presented two-dimensional thirteen nodes element for the analysis of symmetric/unsymmetric cross ply laminated plates. Numerical computation for various examples will be performed. The geometry of the laminated composite plates is shown in Fig. 3. The obtained results will be compared with finite element solutions, wherever available in the literature. In this study, numerical investigations for a couple of symmetric/unsymmetric cross-ply laminated, angle-ply laminated, skew plate laminated, plate strip laminated, simply supported and free edge plates subjected to the transverse sinusoidal loads or uniform transverse load on the top face will be presented. To demonstrate the efficiency of the suggested formulations, a high-precision shear deformable element for the analysis of laminated composite plates of different shapes by Sheikh *et al.* (2002), a C^0-type higher-order theory for bending analysis of laminated composite and sandwich plates by Zhen and Wengi (2010), energy and variational methods in applied mechanics by Reddy (1984), shear locking free robust isoparametric three-node triangular finite element for moderately thick and thin arbitrarily laminated plates by Kabir (1995), an enhanced global-local higher-order theory for the free edge effect in laminates by Lo *et al.* (2007), edge effects of uniformly loaded cross-ply composite laminates by

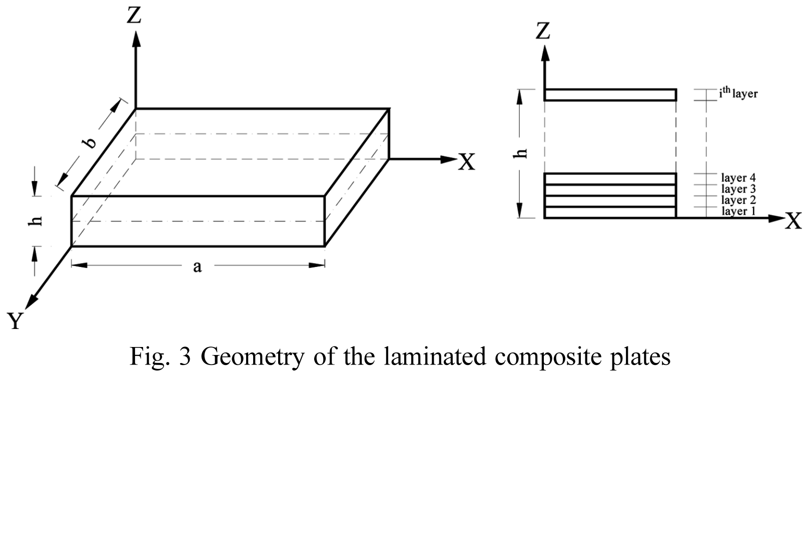

Fig. 3 Geometry of the laminated composite plates

Tahani and Nosier (2003), ending extensional coupling in laminated plates under transverse loading by Whiney (1969), bending of simply supported anti symmetrically laminated rectangular plate under transverse loading by Ren (1987), and the elasticity solutions for cross-ply composite and sandwich laminates by Kant *et al.* (2008), will be compared with the results obtained from the present FE model.

Example 1. *Cross-ply laminate*

A square cross-ply laminated simply supported at the four sides subjected to a sinusoidal transverse loading was considered by Sheikh *et al.* (2002). This plate is analyzed by the proposed element. The elastic constants are chosen as: $E_1 = 25E_2$, $G_{12} = G_{13} = 0.5E_2$, $G_{23} = 0.2E_2$ and $\nu_{12} = 0.25$. The study is made for antisymetric (0°/90°) and symmetric (0°/90°/90°/0°) ply arrangements taking four different values of the span to thickness ratio (*a/h*). Note that the 6×6 and 8×8 mesh are employed to obtain all the results using the proposed element. The deflection and bending moments obtained at the center of the plate are presented in Tables 1 and 2. It can be seen that the obtained responses by the new formulation are in excellent agreement with the high-precision shear deformable element for the analysis of laminated composite plates of different shapes by Sheikh *et al.* (2002), energy and variational methods in applied mechanics by Reddy

Table 1 Deflections at the centre of a simply supported cross-ply square laminate ($1000wE_2h^3/pa^4$)

Stacking sequence	*a/h*	Present analysis with mesh size 6×6	Present analysis with mesh size 8×8	Sheikh *et al.* (2002)	Reddy (1984)	Kabir (1995)
0°/90°	10	19.51	19.16	19.47	19.04	18.95
	48	17.04	17.05	17.04	17.05	17.00
	1000	17.06	16.94	16.95	16.95	16.85
	10000	16.93	16.95	16.95	16.95	16.85
0°/90°/90°/0°	10	9.672	10.03	10.25	9.690	9.660
	48	7.034	6.952	6.987	6.920	6.910
	1000	7.201	6.791	6.797	6.790	6.760
	10000	6.755	6.792	6.797	6.790	6.760

Table 2 Bending moments at the centre of a simply supported cross-ply square laminate ($1000M/pa^2$)

Stacking sequence	*a/h*	Present analysis with mesh size 6×6	Present analysis with mesh size 8×8	Sheikh *et al.* (2002)	Reddy (1984)	Kabir (1995)
0°/90°	10	63.58	62.69	62.68	62.71	62.25
	48	62.02	62.97	62.98	62.98	62.53
	1000	64.19	63.02	63.03	63.00	62.61
	10000	62.69	63.11	63.19	63.00	62.62
0°/90°/90°/0°	10	111.81	112.26	111.35	112.68	111.84
	48	120.23	120.46	120.47	120.51	119.57
	1000	120.57	120.90	120.95	120.93	120.11
	10000	121.42	120.97	121.04	120.93	120.12

(1984), and shear locking free robust isoparametric three-node triangular finite element for moderately thick and thin arbitrarily laminated plates by Kabir (1995). Moreover, it can be easily found that the presented triangular element is suitable for the thin and moderately thick laminated plates and no shear locking to happen in the thin plates ($a/h = 10000$). Besides, in comparison with other researchers, this plate element has a quite rapid rate of convergence for both thin and thick plates because of the using of $w_{,n}$, as an independent degree of freedom.

Example 2. *Cross-ply free-edge laminate*

A free-edge problem in laminates subjected to uniform transverse load on its top surface was considered by Lo *et al.* (2007). The length, width and thickness of the laminated plate are $2a$, $2b$ and h ($a = 5h$, $b = 2h$), respectively. This plate includes two opposite free edges, and two simply supported edges. Each ply is assumed to be of equal thickness, and the material properties used in the present analysis are: $E_1 = 20\times10^6$ psi, $E_2 = E_3 = 2.1 \times 10^6$ psi, $G_{12} = G_{13} = G_{23} = 0.85 \times 10^6$ psi and $\nu_{12} = \nu_{13} = \nu_{23} = 0.21$. Note that the 10×10 meshes are employed to obtain all the results using the proposed element. For easy comparison with other published results, the following non-

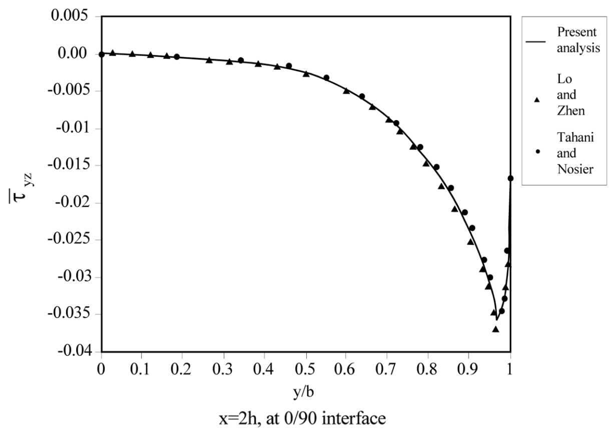

Fig. 4 Inter-laminar shear stresses $\bar{\tau}_{yz}$ across the width in [0°/90°/90°/0°] laminate

Table 3 Non-dimensional inter-laminar shear stresses $\bar{\tau}_{yz}$ across the width in [0°/90°/90°/0°] laminate in $x = 2h$ at 0°/90° interface

Stacking sequence	*y/b*	Present analysis	Lo *et al.* (2007)	Tahani and Nosier (2003)
0°/90°/90°/0° (symmetric)	0.1	00.000	00.000	00.000
	0.2	-0.0006	-0.0006	-0.0006
	0.3	-0.0009	-0.0010	-0.0009
	0.4	-0.00125	-0.00125	-0.00124
	0.5	-0.0025	-0.0027	-0.0024
	0.6	-0.0045	-0.0046	-0.0045
	0.7	-0.0086	-0.0086	-0.0084
	0.8	-0.00144	-0.00148	-0.00142
	0.9	-0.0239	-0.0245	-0.0237

dimensional parameters are considered

$$(\bar{\tau}_{xz}, \bar{\tau}_{yz}) = (\tau_{xy}, \tau_{yz})\frac{h}{q_0 a}$$

The distributions of transverse shear stress $\bar{\tau}_{yz}$ through the width of a [0º/90º/90º/0º] laminate at the mid plane and at the 0º/90º interface are plotted in Fig. 4 and presented in Table 3. Analyzing 4-layered laminated composite plate with the proposed element, gives good answers that are closed to ones from an enhanced global-local higher-order theory for the free edge effect in laminates by Lo *et al.* (2007), and also edge effects of uniformly loaded cross-ply composite laminates by Tahani and Nosier (2003). The findings demonstrate that the higher-order triangular element is a powerful tool to be used for analyzing the laminated composite free-edge plates.

Example 3. *Laminated composite plate strip*

Cylindrical bending of the laminated composite plate strip subjected to a sinusoidal transverse loading $q = q_0\sin(\pi x/a)$ was considered by Zhen and Wanji (2010). The material properties used in this example are: $E_1 = 172.4$ GPa, $E_2 = E_3 = 6.89$ GPa, $G_{12} = G_{13} = 3.45$ GPa, $G_{23} = 1.378$ GPa, and $\nu_{12} = \nu_{13} = \nu_{23} = 0.25$. For easy comparison with other published results, displacements and stresses are normalized in the form bellow

$$\bar{u} = E_2 h^2 u(0,z)/a^3, \quad \bar{\sigma}_x = \sigma_x(a/2,z)h^2/q_0 a^2, \quad \bar{\tau}_{xz} = \tau_{xz}(0,z)/q_0$$

Where a, and h are the length and the thickness of the laminates, respectively. Note that the 12×12 meshes is used to obtain all the results using the proposed element. Distributions of displacement and stress components for unsymmetric four-layer plates [0º/90º/0º/90º] are shown in Figs. 5 and 6 and represented in Tables 4 and 5. The obtained results show good agreement with the C^0-type higher-order theory for bending analysis of laminated composite and sandwich plates by Zhen and Wanji (2010). The results show that the performance of the proposed new element is excellent for analyzing laminated composite plate strip.

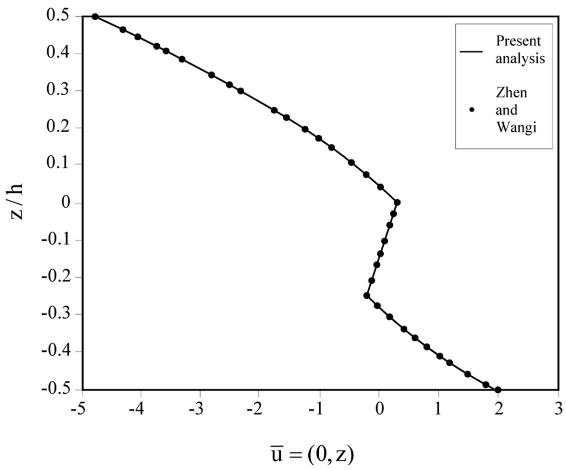

Fig. 5 Distributions of in-plane displacements through the thickness of four-layer plate ($a/h = 4$)

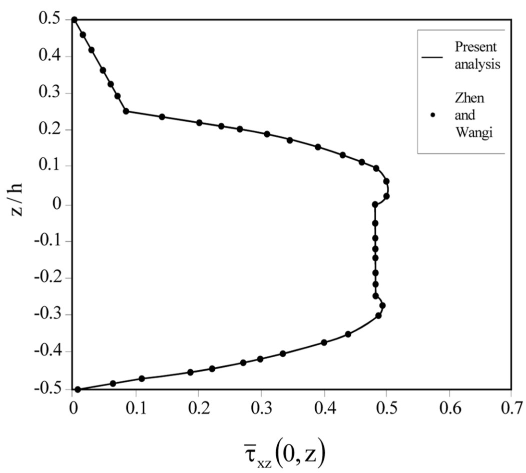

Fig. 6 Distributions of transverse shear stresses through the thickness of four-layer plate ($a/h = 4$)

Table 4 Distributions of in-plane displacements through the thickness of four-layer plate (a/h = 4)

Stacking sequence	z/h	Present analysis	Zhen and Wangi (2010)
0°/90°/0°/90° (unsymmetric)	-0.4	0.901	0.901
	-0.3	0.127	0.127
	-0.2	-0.125	-0.125
	-0.1	0.123	0.124
	0.0	0.291	0.293
	0.1	-0.490	-0.490
	0.2	-1.252	-1.251
	0.3	-2.256	-2.256
	0.4	-3.491	-3.490

Table 5 Distributions of transverse shear stresses through the thickness of four-layer plate (a/h = 4)

Stacking sequence	z/h	Present analysis	Zhen and Wangi (2010)
0°/90°/0°/90° (unsymmetric)	-0.4	0.346	0.348
	-0.3	0.489	0.491
	-0.2	0.484	0.484
	-0.1	0.484	0.484
	0.0	0.484	0.484
	0.1	0.474	0.475
	0.2	0.275	0.278
	0.3	0.068	0.068
	0.4	0.031	0.033

Example 4. *Angle-ply laminate*

A square angle ply ($\theta/-\theta$) antisymmetric laminate simply supported at all the sides subjected to a sinusoidal transverse loading was considered by Sheikh *et al.* (2002). To demonstrate the effectiveness of the suggested formulations, the authors considered various angles for analyzing the laminated plates. In this problem, three degrees of e = 15°, 30° and 45° are used. In all the cases, the thickness ratio (a/h) is taken as 100 and the material properties used in the present analysis are $E_1 = 40E_2$, $G_{12} = G_{13} = 0.5E_2$, $G_{23} = 0.6E_2$ and $\nu_{12} = 0.25$. Note that the 8 × 8 and 12 × 12 meshes are employed to obtain all the results using the proposed element. The results are given in the form of defection and bending moments at the plate centre and axial forces at one of the corners of the plate in Tables 6, 7 and 8. The author's results show good agreement with the high-precision shear deformable element for the analysis of laminated composite plates of different shapes by Sheikh *et al.* (2002), bending extensional coupling in laminated plates under transverse loading by Whitney (1969), and also bending of simply supported anti symmetrically laminated rectangular plate under transverse loading by Ren (1987). To improve the calculation precision, an appropriate selection for the mesh sizes is important. As it can be seen in Tables 6, 7 and 8, using fine mesh for analyzing the plate shows the efficiency of proposed triangular element, especially in solving angle-ply laminated plates.

Table 6 Deflection and stress resultant at the important points of an angle-ply (15º/–15º) square laminate

Deflection and stress resultant	Present analysis with mesh size 8×8	Present analysis with mesh size 12×12	Sheikh *et al.* (2002)	Whitney (1969)	Ren (1987)
$10^3wE_2h^3/pa^4$	7.154	7.166	7.167	7.142	7.169
$10^2N_xh/pa^2$	44.00	44.05	44.10	44.03	44.09
$10^2N_yh/pa^2$	45.62	45.68	45.77	45.67	45.65
$10^2M_xh/pa^2$	11.39	11.42	11.43	11.42	11.42
$10^2M_yh/pa^2$	1.231	1.234	1.234	1.233	1.234

Table 7 Deflection and stress resultant at the important points of an angle-ply (30°/–30°) square laminate

Deflection and stress resultant	Present analysis with mesh size 8×8	Present analysis with mesh size 12×12	Sheikh *et al.* (2002)	Whitney (1969)	Ren (1987)
$10^3wE_2h^3/pa^4$	7.776	7.776	7.770	7.752	7.779
$10^2N_xh/pa^2$	23.29	23.27	23.28	23.21	23.36
$10^2N_yh/pa^2$	30.65	30.65	30.66	30.62	30.66
$10^2M_xh/pa^2$	6.944	6.954	6.953	6.954	6.954
$10^2M_yh/pa^2$	2.682	2.682	2.682	2.681	2.682

Table 8 Deflection and stress resultant at the important points of an angle-ply (45°/–45°) square laminate

Deflection and stress resultant	Present analysis with mesh size 8×8	Present analysis with mesh size 12×12	Sheikh *et al.* (2002)	Whitney (1969)	Ren (1987)
$10^3wE_2h^3/pa^4$	7.336	7.335	7.338	7.321	7.348
$10^2N_xh/pa^2$	4.613	4.623	4.621	4.620	4.650
$10^2N_yh/pa^2$	4.613	4.623	4.621	4.620	4.650
$10^2M_xh/pa^2$	3.679	3.680	3.680	3.680	3.679
$10^2M_yh/pa^2$	3.679	3.680	3.680	3.680	3.679

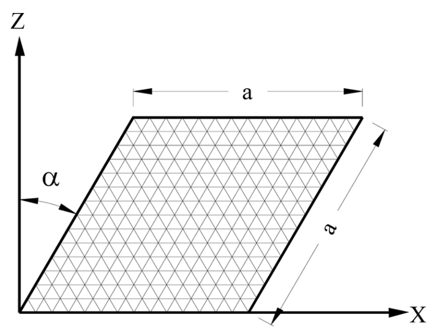

Fig. 7 Geometry of the skew laminated plate

Example 5. *Skew laminate*

A skew laminated plate simply supported at all the sides subjected to a sinusoidal transverse loading, with the span to the thickness ratio (*a/h*) as 10 was considered by Sheikh *et al.* (2002). The elastic constants are chosen as: $E_1 = 25E_2$, $G_{12} = G_{13} = 0.5E_2$, $G_{23} = 0.2E_2$ and $\nu_{12} = 0.25$. The study is made for skew angle of 15°, 30° and 45° taking cross-ply (0°/90°/0°) and angle-ply (45°/–45°/45°) arrangements. Note that the 10 × 10, 12 × 12 and 14 × 14 meshes are employed to obtain all the results using the proposed element. Geometry of the skew laminated plate is shown in Fig. 7. The defection and bending moments obtained at the plate centre are presented in Tables 9, 10 and 11. Obtained numerical results, using this element, agree well with the high-precision shear deformable element for the analysis of laminated composite plates of different shapes by Sheikh *et al.* (2002). Moreover, this plate element has a quite rapid rate of convergence.

Table 9 Deflection and bending moments at the center of a simply supported skew composite plate with skew angle (15°)

Deflection and stress resultant	Present analysis with mesh size			Sheikh *et al.* (2002)
	10×10	12×12	14×14	
Cross-ply (0°/90°/0°)				
$10^3 wE_2h^3/pa^4$	9.711	9.728	9.740	9.743
$10^3 M_x/pa^2$	118.39	118.47	118.50	118.49
$10^3 M_y/pa^2$	13.38	13.46	13.47	13.47
Angle-ply (45°/–45°/45°)				
$10^3 wE_2h^3/pa^4$	9.183	9.264	9.277	9.277
$10^3 M_x/pa^2$	45.92	46.02	46.11	46.10
$10^3 M_y/pa^2$	47.95	48.01	48.05	48.05

Table 10 Deflection and bending moments at the center of a simply supported skew composite plate with skew angle (30°)

Deflection and stress resultant	Present analysi with mesh sizes			Sheikh *et al.* (2002)
	10×10	12×12	14×14	
Cross-ply (0°/90°/0°)				
$10^3 wE_2h^3/pa^4$	8.052	8.191	8.195	8.195
$10^3 M_x/pa^2$	99.98	100.08	100.11	100.10
$10^3 M_y/pa^2$	14.77	14.83	14.90	14.90
Angle-ply (45°/–45°/45°)				
$10^3 wE_2h^3/pa^4$	8.306	8.399	8.420	8.417
$10^3 M_x/pa^2$	46.60	46.67	46.73	46.73
$10^3 M_y/pa^2$	50.52	50.59	50.62	50.64

Table 11 Deflection and bending moments at the center of a simply supported skew composite plate with skew angle (45°)

Deflection and stress resultant	Present analysis with mesh size			Sheikh *et al.* (2002)
	10×10	12×12	14×14	
Cross-ply (0°/90°/0°)				
$10^3 wE_2h^3/pa^4$	5.402	5.496	5.511	5.513
$10^3 M_x/pa^2$	67.59	67.71	67.73	67.73
$10^3 M_y/pa^2$	14.94	15.03	15.19	15.20
Angle-ply(45°/–45°/45°)				
$10^3 wE_2h^3/pa^4$	5.397	5.488	5.492	5.490
$10^3 M_x/pa^2$	38.92	38.96	39.00	39.00
$10^3 M_y/pa^2$	43.44	43.48	43.55	43.55

Table 12 Comparison of maximum stresses for square sandwich plate

a/h	Stress components	Present analysis with mesh size		Zhen and Wangi (2010)	Kant *et al.* (2008)
		6×6	12×12		
For *a/h* = 4					
	$\bar{\sigma}_x(0,0,h/2)$	1.5643	1.5651	1.5622	1.5660
	$\bar{\sigma}_x(0,0,-h/2)$	-1.5643	-1.5651	-1.5622	-1.5120
	$\bar{\sigma}_y(0,0,h/2)$	0.2523	0.2552	0.2549	0.2590
	$\bar{\sigma}_y(0,0,-h/2)$	-0.2523	-0.2552	-0.2549	-0.2590
	$\bar{\tau}_{xz}(a/2,0,0)$	0.2373	0.2379	0.2372	0.2390
	$\bar{\tau}_{yz}(0,b/2,0)$	0.1051	0.1054	0.1050	0.1070
For *a/h* = 10					
	$\bar{\sigma}_x(0,0,h/2)$	1.150	1.155	1.1686	1.1530
	$\bar{\sigma}_x(0,0,-h/2)$	-1.150	-1.155	-1.1686	-1.1520
	$\bar{\sigma}_y(0,0,h/2)$	0.1109	0.1113	0.1117	0.1100
	$\bar{\sigma}_y(0,0,-h/2)$	-0.1109	-0.1113	-0.1117	-0.1100
	$\bar{\tau}_{xz}(a/2,0,0)$	0.2933	0.2956	0.2957	0.3000
	$\bar{\tau}_{yz}(0,b/2,0)$	0.0506	0.0510	0.0506	0.0527
For *a/h* = 20					
	$\bar{\sigma}_x(0,0,h/2)$	1.1100	1.1102	1.1101	1.1100
	$\bar{\sigma}_x(0,0,-h/2)$	-1.1100	-1.1102	-1.1101	-1.1100
	$\bar{\sigma}_y(0,0,h/2)$	0.0691	0.0700	0.0697	0.0700
	$\bar{\sigma}_y(0,0,-h/2)$	-0.0691	-0.0700	-0.0697	-0.0700
	$\bar{\tau}_{xz}(a/2,0,0)$	0.3168	0.3173	0.3174	0.3170
	$\bar{\tau}_{yz}(0,b/2,0)$	0.0360	0.0360	0.0360	0.0360

Example 6. *Sandwich plate*

Simply-supported three-layer sandwich plate subjected to a doubly sinusoidal transverse loading $q = q_0\sin(\pi x/a)\sin(\pi y/b)$ was considered by Zhen and Wanji (2010). The following non-dimensional stress components are considered for comparison with other published results:

$$\bar{\sigma}_x = \sigma_x h^2/q_0 a^2, \quad \bar{\tau}_{xz} = \tau_{xz} h/q_0 a, \quad \bar{\tau}_{yz} = \tau_{yz} h/q_0 a$$

The thickness of face sheets at the upper and the lower surfaces equals to 0.1 h, whereas the thickness of core is of 0.8 h. For the sandwich plate, the material properties for face sheet are $E_1 = 172.4$ GPa, $E_2 = E_3 = 6.89$ GPa, $G_{12} = G_{13} = 3.45$ GPa, $G_{23} = 1.378$ GPa, and $\nu_{12} = \nu_{13} = \nu_{23} = 0.25$. The elastic constants for core are $E_1 = E_2 = 0.276$ GPa, $E_3 = 3.45$ GPa, $G_{13} = G_{23} = 0.414$ GPa, $G_{12} = 0.1104$ GPa, and $\nu_{12} = \nu_{13} = \nu_{23} = 0.25$. Note that the 6 × 6 and 12 × 12 meshes are employed to obtain all the results using the proposed element. The stress components obtained from the present analysis for three-layer sandwich plate are represented in Table 12. The calculated results are in excellent agreement with the C^0-type higher-order theory for bending analysis of laminated composite and sandwich plates by Zhen and Wanji (2010), and also the elasticity solutions for cross-ply composite and sandwich laminates by Kant *et al.* (2008). This finding highlights the capability of new formulation for analyzing sandwich plates. It should be mentioned again, using of $w_{,n}$, as an independent degree of freedom in new higher-order element shows a quite rapid rate of convergence.

4. Conclusions

An efficient two-dimensional thirteen nodes triangular plate bending element with transverse shear effect is formulated. This new element is based on the higher-order shear deformation theory, and it is suitable for the analysis of thin and moderately thick laminated composite plate. Unlike other presented plate elements, the proposed formulations do not contain any parameter without physical meaning and the boundary conditions at the top and also bottom surfaces of the structure are exactly satisfied. In addition, due to the high-order of the different interpolation functions for transverse displacement and bending rotations, new element is free from any transverse shear locking and spurious modes. From the application point of view, it has a quite rapid rate of convergence for the analysis of both thin and thick plates. In fact, using $w_{,n}$ as a degree of freedom with independent interpolation function, is very effective to obtain accurate answers and accelerated the rate of convergence. This study offers very good numerical results for the orthotropic laminated composite plates with different structural parameters, such as boundary conditions, shapes, number of layers, thickness ratios and fiber orientations. Furthermore, the findings highlighted the capability of the suggested formulation to estimate accurately the values of the stresses and deflections.

References

Alieldin, S.S., Alshorbagy, A.E. and Shaat, M. (2011), "A first-order shear deformation finite element model for elastostatic analysis of laminated composite plates and the equivalent functionally graded plates", *Ain Shams Eng. J.*, **2**, 53-62.

Belinha, J. and Dinis, L.M.J.S. (2006), "Analysis of plates and laminates using the element free Galerkin method", *Comput. Struct.*, **84**, 1547-1559.

Belounar, L. and Guenfoud, M. (2005), "A new rectangular finite element based on the strain approach for plate bending", *Thin Wall. Struct.*, **43**, 47-63.

Bussamra, F.L.S., Neto, E. and Raimundo, D.S. (2012), "Hybrid quasi-Trefftz 3-D finite elements for laminated composite plates", *Comput. Struct.*, **92-93**, 185-192.

Cai, Y.C., Zhu, H.H. and Guo, S.Y. (2008), "The elastoplastic formulation of polygonal element method based on triangular finite meshes", *Struct. Eng. Mech.*, **30**(1), 119-129.

Carrera, E., Miglioretti, F. and Petrolo, M. (2011), "Accuracy of refined finite elements for laminated plate analysis", *Compos. Struct.*, **93**, 1311-1327.

Carrera, E., Miglioretti, F. and Petrolo, M. (2011), "Guidelines and recommendations on the use of higher order finite elements for bending analysis of plates", *Int. J. Comput. Meth. Eng. Sci. Mech.*, **12**, 303-324.

Cen, S., Long, Y. and Yao, Z. (2002), "A new hybrid-enhanced displacement-based element for the analysis of laminated composite plates", *Comput. Struct.*, **80**, 819-833.

Kabir, H.R.H. (1995), "A shear locking free robust isoparametric three-node triangular finite element for moderately thick and thin arbitrarily laminated plates", *Comput. Struct*., **57**, 589-597.

Kant, T., Gupta, A.B., Pendhari, S.S. and Desai, Y.M. (2008), "Elasticity solution for cross-ply composite and sandwich laminates", *Compos. Struct.*, **83**, 13-24.

Lo, S.H., Zhen, W., Cheung, Y.K and Wanji, C. (2007), "An enhanced global-local higher-order theory for the free edge effect in laminates", *Compos. Struct.*, **81**, 499-510.

Mindlin, R.D. (1951), "Influence of rotatory inertia and shear deformation on flexural motions of isotropic elastic plates", *ASME. J. Appl. Mech.*, **18**, 31-38.

Padmanav, Dash. and Singh, B.N. (2010), "Geometrically nonlinear bending analysis of laminated composite plate", *Commun. Nonlin.. Sci. Numer. Simul*., **15**, 3170-3181.

Polit, O. and Touratier, M. (2000), "High-order triangular sandwich plate finite element for linear and non-linear analyses", *Comput. Meth. Appl. Mech. Eng.*, **185**, 305-324.

Reddy, J.N. (1984), "A simple higher-order theory for laminated composite plates", *Appl. Mech. ASME*., **51**, 745-752.

Reddy, J.N. (1984), *Energy and Variational Methods in Applied Mechanics*, Wiley, New York.

Reddy, J.N. (1997), *Mechanics of Laminated Composite Plates Theory and Analysis*, Boca Raton, CRC Press.

Reissner, E. (1945), "The effect of transverse shear deformation on the bending of elastic plates", *ASME. J. Appl. Mech.*, **12**, A69-77.

Ren, J.G. (1987), "Bending of simply supported anti symmetrically laminated rectangular plate under transverse loading", *Compos. Sci. Technol.*, **28**, 231-243.

Rezaiee-Pajand, M. and Akhtary, M.R. (1996), "Study of several six-node plate bending triangular elements", *Journal of Faculty of Engineering*, *University of Tabriz*, **15**, 17-38. (in Persian)

Rezaiee-Pajand, M. and Akhtary, M.R. (1998), "A family of 13-node plate bending triangular elements", *Commun. Numer. Meth. Eng.*, **14**, 529-537.

Rezaiee-Pajand, M. and Sarafrazi, S.R. (2000), "Including the shear deformation in thin plate bending and beam elements", *Amirkabir J. Sci. Technol.*, **42**(11), 130-147. (in Persian)

Rezaiee-Pajand, M. and Mohamadzade, H.R. (2010), "Finite element template for four-sided kirchhoff plate bending", *Journal of civil and environmental Engineering, University of Tabriz*, **2**(40), 25-38. (in Persian)

Rezaiee-Pajand, M. and Karkon, M. (2012), "Two efficient hybrid-Trefftz elements for plate bending analysis", *Latin Am. J. Solids Struct*., **9**(1).

Rolfes, R. and Rohwer, K. (1997), "Improved transverse shear stresses in composite finite elements based on first order shear deformation theory", *Int. J. Numer. Meth. Eng.*, **40**, 51-60.

Rolfes, R., Rohwer, K. and Ballerstaedt, M. (1998), "Efficient linear transverse normal stress analysis of layered composite plates", *Comput. Struct*., **68**, 643-652.

Sheikh, A.H., Haldar, S. and Sengupta, D. (2002), "A high precision shear deformable element for the analysis of laminated composite plates of different shapes", *Compos. Struct.,* **55**, 329-336.

Sheikh, A.H. and Chakrabarti, A. (2003), "A new plate bending element based on higher-order shear deformation theory for the analysis of composite plates", *Finite Elem. Analy. D.*, **39**, 883-903.

Tahani, M. and Nosier, A. (2003), "Edge effects of uniformly loaded cross-ply composite laminates", *Mater.*

Des., **24**, 647-658.
Thinh, T.I. and Quoc, T.H. (2010), "Finite element modeling and experimental study on bending and vibration of laminated stiffened glass fiber/polyester composite plates", *Comput. Mater. Sci.*, **49**, S383-S389.
Timoshenko, S. and Krieger, S.W. (1995), *Theory of Plates and Shells*, 2nd Edition, McGraw-Hill, Singapore.
Tu, T.M., Thach, L.N. and Quoc, T.H. (2010), "Finite element modeling for bending and vibration analysis of laminated and sandwich composite plates based on higher-order theory", *Comput. Mater. Sci.*, **49**, S390-S394.
Vlachoutsis, S. (1992), "Shear correction factors for plates and shells", *Int. J. Numer. Meth. Eng.*, **33**, 1537-1552.
Whitney, J.M. (1969), "Bending extensional coupling in laminated plates under transverse loading", *J. Compos. Mater.*, **3**, 20-35.
Zhen, W. and Wanji, C. (2010), "A C^0-type higher-order theory for bending analysis of laminated composite and sandwich plates", *Compos. Struct.*, **92**, 653-661.

Notations

u, v	: In-plane displacement components at the nodes
w	: Transverse displacement at the nodes
u_0, v_0, w_0	: Displacement components at the midplane
$w_{,x}$, $w_{,y}$, $w_{,n}$	: Partial derivatives of w with respect to x, y and n
n, t	: Normal and tangential vectors
θ_x, θ_y	: Rotation of normals to midplane
$[N_1]$, $[N_2]$	: Interpolation function matrices
$\{\alpha\},\{\beta\},\{\gamma\},\{\lambda\},\{\mu\},\{\psi\}$	: Unknown coefficient vectors
ξ_i, ξ_j, ξ_k	: Dimensionless vectors
$\{\delta\}$	: Nodal displacement vector
$[A]$	: Formed with the coordinates of the different nodes
$\{\Delta\}$	: Total unknown coefficient vectors
φ_j	: Angle between n_j and x axis
x_j, y_j	: Coordinates of node j
ϕ_x, ϕ_y	: Average transverse shear strain components
$\{\varepsilon\}$	: Strain vector
$\{\varepsilon_b\}$	: In-plane strain vector
$\{\varepsilon_s\}$	: Transverse shear strain vector
$\{\sigma\}$	: Stress vector
$\{\sigma_b\}$	: In-plane stress vector
$\{\sigma_s\}$	: Transverse shear stress vector
z	: Distance from midplane
$[Q_b]$	: The transformed material constants for bending
$[Q_s]$	: The transformed material constants for shear
$[D]$	: Rigidity matrix of the laminate
$[D_b]$	: Rigidity matrix of the laminate due to bending
$[D_s]$	: Rigidity matrix of the laminate due to shear
$[B]$	: Strain displacement matrix
$[K]$	: Element stiffness matrix
V	: Potential energy
$\{P\}$	: Nodal load vector
a	: Length of the plate
b	: Width of the plate
h	: Thickness of the plate
E_i	: Young's modulus of elasticity
G_{ij}	: Shear modulus of elasticity
v_{ij}	: Poisson's ratio